ACS OMEGA

Article

Cite This: ACS Omega 2018, 3, 2049−2057

Magnetic Two-Way Valves for Paper-Based Capillary-Driven Microfluidic Devices

Mario Fratzl,[†,‡] Boyce S. Chang,[§] Stephanie Oyola-Reynoso,[§] Guillaume Blaire,[†] Sarah Delshadi,[†,∥] Thibaut Devillers,[‡] Thomas Ward, III,[⊥] Nora M. Dempsey,[‡] Jean-Francis Bloch,[*,#] and Martin M. Thuo[*,§]

[†]Univ. Grenoble Alpes, CNRS, Grenoble INP, Institute of Engineering, G2Elab, 38000 Grenoble, France

[‡]Univ. Grenoble Alpes, CNRS, Grenoble INP, Institute of Engineering, Institut Néel, 38000 Grenoble, France

[§]Department of Materials Science and Engineering and [⊥]Department of Aerospace Engineering, Iowa State University, Ames, Iowa 50011, United States

[∥]Univ. Grenoble Alpes, CNRS, Inserm, IAB, 38000 Grenoble, France Site Santé—Allée des Alpes, 38700 La Tronche, France

[#]Univ. Grenoble Alpes, CNRS, Grenoble INP, Institute of Engineering, 3SR, F-38000 Grenoble, France

Supporting Information

ABSTRACT: This article presents a magnetically actuated two-way, three-position (+, 0, −), paper-based microfluidic valve that includes a neutral position (0)—the first of its kind. The system is highly robust, customizable, and fully automated. The advent of a neutral position and the ability to precisely control switching frequencies establish a new platform for highly controlled fluid flows in paper-based wicking microfluidic devices. The potential utility of these valves is demonstrated in automated, programmed, patterning of dyed liquids in a wicking device akin to a colorimetric assay but with a programmed fluid/reagent delivery. These valves are fabricated using facile methods and thus remain cost-effective for adoption into affordable point-of-care/bioanalytical devices.

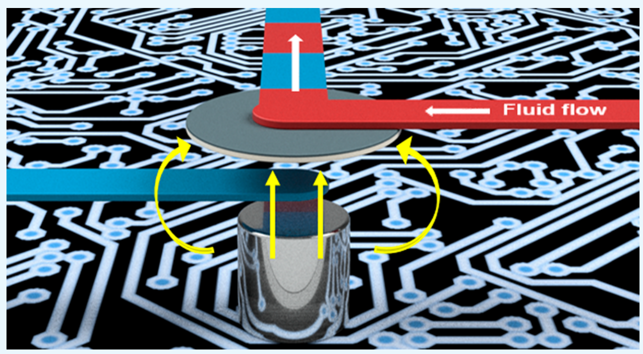

■ INTRODUCTION

Affordable microfluidics has recently garnered renewed interest, in part, because of the emergence of pump-free, capillary wicking-based point-of-care (PoC)/bioanalytical devices. These devices allow users to perform chemical and biochemical sensing beyond what is currently available in most laboratory environments. PoC devices need to be low cost and deliver rapid results and be simple to use even by unskilled personnel, irrespective of the setting.[1,2] Although pump-free and wicking-based analytical devices (e.g., pregnancy tests) have been used for a long time, a resurgence in interest has occurred following the introduction of microfluidic paper analytical devices (μPADS) in 2007.[3] μPADS offer simple, disposable, and affordable analytical devices for bioassays and environmental analysis.[4−12] These μPADS have numerous advantages over classical microfluidics: (i) porosity-induced capillary action eliminates the need for external pumps, (ii) μPADS are biocompatible for various applications including clinical diagnosis, food quality control, and environmental monitoring, and[13] (iii) μPADS and paper microfluidics are built upon established technologies such as lateral flow tests.

A downside to this promising technology is the reproducibility of the active elements used in conventional open-channel microfluidic applications—assuring a robust fluid control, such as valves and switches. This challenge has led to an intense search for methods to control fluidic flows on wicking-based devices. Recently, efforts to fabricate paper-based valves to switch fluid flows on and/or off in channels have been reported. These valves fall into two main categories: (i) wetting-based gating, where the wettability of the barrier changes in the presence of a stimulus or (ii) controlling the contact between two wicking channels. One approach is based on hydrophobic and hydrophilic electrodes that close and open a fluidic channel when a voltage is applied. In the valve concept presented by Koo et al. in 2013,[14] the fluid flows past a hydrophilic electrode and stops at the hydrophobic electrode (Figure 1a(i)). When a voltage is applied, the hydrophobic layer is destroyed and fluid flow is triggered. A similar valve based on melting wax has also been developed.[15] Electrowetting or thermal gating valves are destructive and are one-way single-use (actuation can only be performed once) devices.[16,17] Furthermore, there is no guarantee that the applied voltages/heat or degraded chemicals will not affect the analyte or the fluidic properties. As an alternative, Chen et al.[18] exploited the biphilic nature of

Received: November 22, 2017
Accepted: February 1, 2018
Published: February 20, 2018

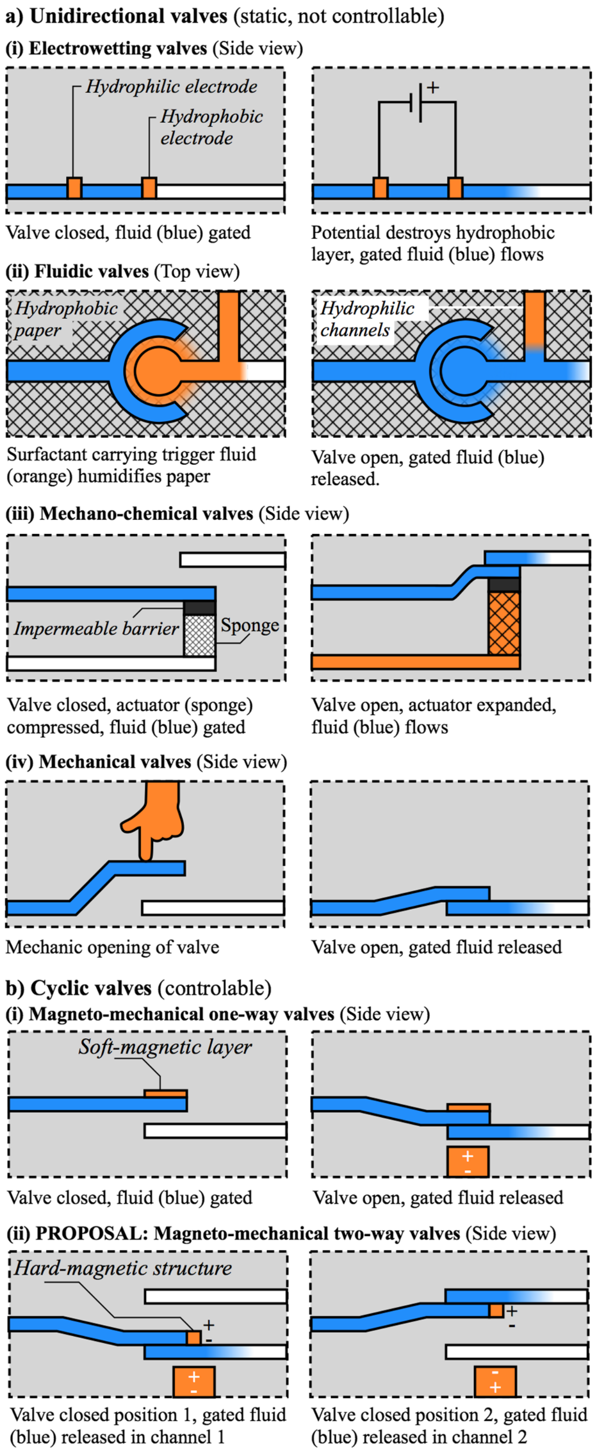

Figure 1. (a) Approaches for unidirectional valves. These methods are generally irreversible and difficult to control. (b) Controlled and reversible valves using magnetomechanical actuation.

surfactants to invert the wettability of a nonwetting gate allowing fluid flow. The valve consists of a disk (trigger) and an open ring surrounding the trigger as a gate, both separated by a hydrophobic gap (Figure 1a(ii)). A trigger fluid (orange) loaded with surfactants helps overcome the hydrophobic gate allowing an aqueous fluid flow. The dissolved surfactant molecules raise the surface tension of the hydrophobic barrier, releasing the gated fluid (blue). This approach, however, introduces the surfactant into the test fluid, increasing the flow and test complexity. Houghtaling et al.[19] reported a soluble bridge-type valve, where a short piece of the μPAD can be dissolved, opening the valve.

The main class of paper fluidic valves, however, is mechanically triggered valves in which the contact between two channels is controlled. Toley et al. recently reported an actuation-based valve using paper strips and fluid-triggered expanding elements (swelling sponge) to push two channels into contact (Figure 1a(iii)).[20] A similar two-way valve, based on a fluid-triggered paper actuator, has recently been presented by Kong et al.[21] Other mechanically triggered valves are mostly based on manual actuation of a paper cantilever (Figure 1a(iv)).[22−26] Each of these techniques has their unique advantages and disadvantages with regards to cost, automation, flexibility in design, and reliability. In general, most of the presented techniques are either irreversible (one way)[14,18,23] or have a slow switching dynamics.[20,22,24,25] Of all presented systems, only the fluid-triggered expanding element valves[20,21] allow switching between two exit channels. Furthermore, the response dynamics would be slow and erratic because the switching mechanism depends on polymer swelling or paper deformation kinetics.

Magnetism is widely used in microfluidics to exert contactless and long-range attractive or repulsive forces on ferromagnetic, ferrimagnetic, or paramagnetic materials. Li et al.[27] reported a paper-based magnetomechanical valve fabricated by attaching an iron-loaded polydimethylsiloxane (PDMS) film on one side of a paper cantilever (Figure 1b(i)). By applying an external magnetic field, the cantilever deforms and comes in contact with an underlying channel, allowing the fluid to flow downstream, thus providing a reversible valve actuation. However, this method has numerous limitations, the principle one of which is the use of soft magnetic nanoparticles which implies that only attractive magnetic forces can be used to close the valve. As the magnetic film covers one side of the paper cantilever, fluid flow can only be achieved through the opposite side, limiting the channel capacity and eliminating the possibility of two-way valves. In summary, a majority of the reported valves are, therefore, one-way and/or slow in actuation and hence are comparable to an electric diode (applying electrical circuit theory to microfluidics).[28−30] To build logic-based (programmable) systems comparable to conventional microfluidics from paper-based devices, the equivalent of multiway switches and transistors is needed.

Recently, we developed techniques to micropattern high-performance hard magnetic polymer composites based on magnetic powders[31] or pillars,[32] characterized by magnetic field gradients as high as 10^6 T/m. Paper−polymer composites are also well-known, and permeation of polymeric materials into paper has been reported.[33] Building on this success, we hypothesized that integrating spatially resolved controlled wetting (hydrophobic and hydrophilic zones) coupled with patterned hard magnets on paper will lead to a three-point, two-way valve for wicking-based (filled channel) microfluidic devices. Herein, we demonstrate that hard magnetic powders such as NdFeB can be directly incorporated into paper (Figure 1b(ii)) to create a highly customizable (hackable and stackable) two-way valve. In this case, both paper surfaces remain available for capillary fluid transport and following magnetization of the hard magnetic powder, the cantilever can attract or repel the paper by applying a magnetic field and hence, switching the valve. This allows for the first magnetic-μPAD (M-μPAD) compatible two-way valve. We present two adaptable methods

DOI: 10.1021/acsomega.7b01839
ACS Omega 2018, 3, 2049−2057

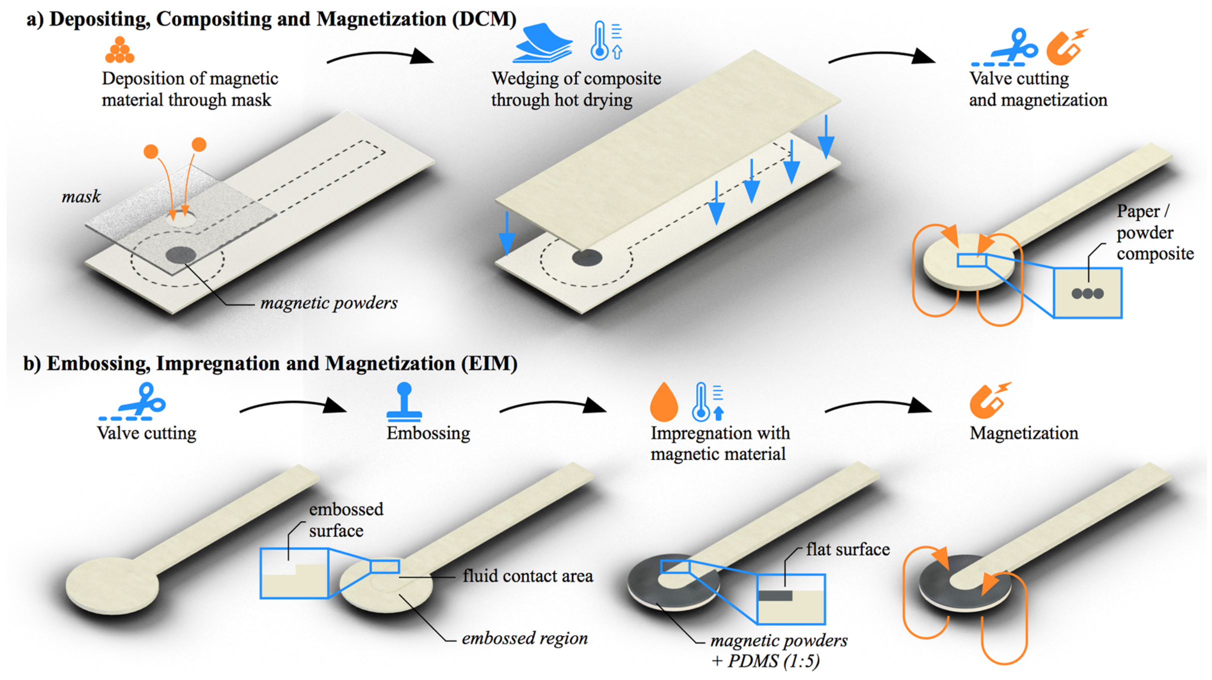

Figure 2. (a) The DCM method is predicted to be more suitable for large-scale production because the magnetic powder is embedded during the fabrication of paper. (b) EIM method represents a more general route of making magnetic valves.

to fabricate such a device, each being expandable to a variety of valve designs or platforms.

■ VALVE DESIGN AND FABRICATION

To obtain a functional paper magnetic valve, both surfaces of the paper must remain accessible for capillary fluid transport. Ideally, both capillary surfaces have the same size to guarantee a consistent fluid flow. Furthermore, the magnetic particles should be isolated from the moving liquid to avoid contamination of the analyte, degradation of the magnetic particles, and/or unwanted reactions. We present two different techniques to build paper magnetic valves (Figure 2). For brevity and clarity, we designate these two approaches as follows: (i) depositing, compositing, and magnetization (abbreviated DCM, Figure 2a) and (ii) embossing, impregnation, and magnetization (abbreviated EIM, Figure 2b) techniques. Note that both techniques offer full flexibility to design the valve geometry and the magnetoactive zone(s) depending on the application. In this work, we chose valves that consist of a disk pad (15 mm diameter) attached to a rectangular test strip (5 × 25 mm). Magnetoactive zones were shaped as disks, open rings, and squares. These magnetoactive zones were isolated or fixed onto paper using PDMS. To mitigate reagent adsorption into the polymer matrix, a trichloro perfluoroalkylsilane hydrophobic barrier was drawn between the wicking channel and the deposited magnetoactive zone.[34] The PDMS matrix can be replaced with other polymers such as super glue or wax; however, the integrity of the microfluidic channel may be compromised depending on the wetting/wicking properties of the polymer (see superglue example, Figure S1).[35,36] Viscous liquid polymers, such as precured PDMS or molten wax, minimally spread in the lateral direction but still get imbibed through the thickness of the paper, primarily because of gravity.[37−39] The higher viscosity also aids in the dispersion of particles during mixing; therefore, a more homogeneous substrate is obtained. For easier processing and device fabrication, the particles were magnetized after device fabrication.

Depositing, Compositing, and Magnetization. The DCM technique was developed to allow a large-scale production of paper magnetic valves. Therefore, the magnetoactive regions were directly integrated during the paper fabrication process. After fabricating a sheet of paper through an ISO 5269/1 TAPPI process, the outline of the valve was traced using a pen on the still-wet sheet (Figure 2a). Hard magnetic powders were deposited through a transparent polyethylene terephthalate mask to form the magnetoactive zone. Figure 2a shows the fabrication of a disk-shaped magnetoactive zone; however, the shape of the zone can be adapted to any need. A second sheet of the paper with identical properties was fabricated and placed on the first one. The composite structure was subsequently dried in a sheet dryer at 60 °C. This compound paper was stable, and the process does not require additional chemical binders. Further reinforcement of the magnetic particles, if needed, can be attained by adding ca. 0.01 g of PDMS through the magnetoactive zones, which upon curing (30 min curing time at 80 °C) will subsequently coat and reinforce the fiber network, isolating the magnetic particles from the flowing fluid.

Embossing, Impregnation, and Magnetization. Although the DCM technique is suitable for scale-up and rapid prototyping, the TAPPI process is not readily accessible, especially in resource-limited settings. The EIM technique consists of a selective deposition of the magnetic powder on the valve, such that the position of the particles does not affect the fluidic flow through the channel nor interfere with the analyte. First, the valve is cut out of a sheet of paper followed by partial embossing of a C ring shape around the valve zone to aid in the deposition of the magnetic particles (Figure 2b). From embossing, a step (80 ± 20 μm) designating the magnetoactive region was created using a three-dimensionally printed mold (Figure S2). Hard magnetic particles (NdFeB) dispersed in

DOI: 10.1021/acsomega.7b01839
ACS Omega 2018, 3, 2049−2057

PDMS (mass ratio of 5:1 PDMS/NdFeB) were then deposited on the embossed region. Suspension (0.05 g) was used per device. The PDMS matrix wicks through the paper and upon curing, immobilizes the particles in place without compromising the channel portion of the device (Figure 2b).

Theoretical Understanding of Flow Behavior in Paper. Fluid transport in paper has been qualitatively investigated and depends on the uniform surface chemistry and fiber uniformity and follows transport behavior in porous media.[40] For clarity and predictability, we empirically and in silico-evaluated fluidic transport in our paper to assess for the predictability of fluid behavior (see Supporting Information, Figure S8). For a pulsed flow using the valves proposed herein, there should be two asymptotic time domains that can be used to separate mixing from slug formation. The two dominant time domains are the asymptotic physical limits of molecular diffusion and momentum transport. Fluid flow in porous media is typically governed by Darcy's law which results in a reduced-order momentum equation that is based on an average fluid velocity, u, and is of the form[40,41]

$$u = -(K/\mu)\nabla P$$

Here, μ denotes the viscosity of the fluid and, K, is typically the Darcy flow permeability. Assuming a unidirectional motion and homogeneous permeability, the equation may be integrated to determine an expression for the pressure that drives fluid motion. It is generally understood that fluid motion in fiber-based porous media is driven by a combination of capillary pressure, that is, the wettability of the fluid on the fibers, and the porosity, here denoted using ε. A general form of the equation for capillary pressure is

$$P_{cap} = -f(\varepsilon)\gamma \cos\theta/a$$

That is, measuring the capillary pressure involves some direct measurement of contact angle θ and surface tension, γ. Here, we write the function denoting porosity as $f(\varepsilon) = (1-\varepsilon)/\varepsilon$ such that materials with a high porosity will tend to have a lower capillary pressure.[40] The negative sign yields a vacuum gauge pressure relative to a reference one which we take here to be zero. The last variable, a, represents a length scale of the capillary pressure which is typically considered to be the hydraulic fiber radius which we take to be half a typical fiber width (~20 μm).[42] In practice, it is simpler to lump the capillary pressure as a single term because measuring the parameters independently is difficult. Furthermore, there is a direct relationship between the permeability and porosity for paper-based porous media.[42] Inserting the capillary pressure as the boundary condition for Darcy flow over the arbitrary distance, $L(t)$, and then noting that the unidirectional velocity at the interface is $u = \mathrm{d}L/\mathrm{d}t$ results in a familiar rate equation for the distance traveled or $L(t) = [2tKf(\varepsilon)\gamma \cos\theta/a\mu]^{1/2}$. Note that this expression is similar to the reduced order form of the Lucas–Washburn expression for capillary rise in a vertical tube, that is, $L \approx t^{1/2}$.[43,44] The rate of mass transport is proportional to $\omega_{diff} = D/[(1-\varepsilon)t]^2$, where D is the diffusivity, t is the paper thickness, and $(1-\varepsilon)t$ is the length occupied by the paper. Valve pulse frequencies greater than this will always lead to the mixing of two miscible fluids in the fiber channels. Similarly, when the valve frequency is less than the displacement frequency $\omega_{disp} = 2Kf(\varepsilon)\gamma \cos\theta/\mu aL^2$, where L is the desired distance traveled by the fluid, slug formation occurs. It is therefore feasible to exploit actuation to introduce mixed or sequential bands of liquids in a paper channel. This implies that microfluidic mixers on capillary-driven channels can be realized or sequences of liquid plugs akin to droplets of oil in water in regular microfluidics can be obtained.

■ RESULTS AND DISCUSSION

All fabricated devices were evaluated for integrity by wicking a colored aqueous fluid through the microfluidic channel. The papers used in this work are fabricated in-house with no additives, hence isolating their effect on the valve performance. Figure 3a shows a fabricated DCM valve integrated into a M-μPAD, with the trapped hard magnetic particles visible through the composite structure. The TAPPI process-fabricated paper had a thickness of 149 ± 3 μm (per single sheet), a basis weight of 120.5 g/m^2, and a porosity of 0.47; thus, the composite had a total thickness of 291 ± 3 μm. The structure was magnetized in

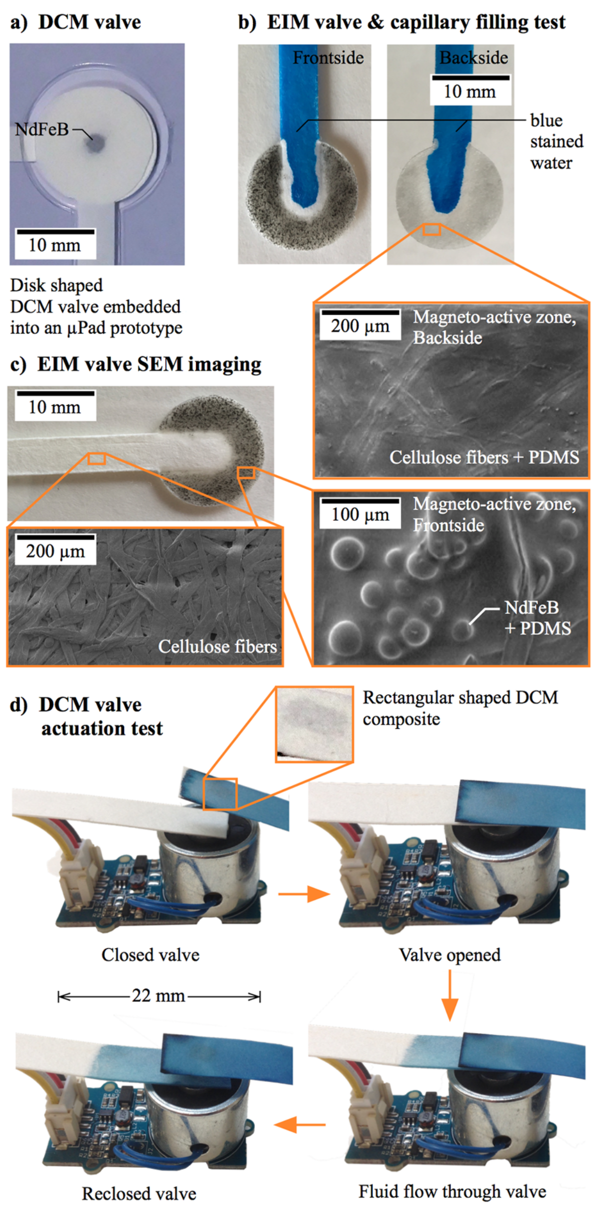

Figure 3. (a) Prototype of a DCM valve. (b) EIM prototype valve with the fluid flowing only in the test channels. (c) SEM images of selected areas in the EIM valve showing the impregnation of PDMS and the magnetic particles on the paper. (d) Successful demonstration of a DCM valve actuation test.

DOI: 10.1021/acsomega.7b01839
ACS Omega 2018, 3, 2049–2057

the out-of-plane direction under an applied magnetic field of 1.5 T. A stray field out-of-plane component of 3.0 ± 0.2 mT was measured at 1.5 mm above the magnetoactive surface.

Similarly, Figure 3b shows a fabricated EIM device (fabricated out of blotting paper) with the fluidic channel holding blue colored water. The magnetoactive zone does not wet and is therefore isolated from the channel (Figure 3b). A scanning electron microscopy (SEM) image of the dispersed particles (Figure 3c) showed a stochastic distribution in the matrix; hence, a Gaussian distribution of the magnetic field strength is expected across the magnetoactive zone. Imaging the backside of the magnetoactive zone reveals no particles, although the PDMS matrix is shown to have permeated through. Comparing the backside of this device with an untreated region shows that although the fiber organization is not perturbed by the deposition process, the porosity is however significantly different because of the presence of the matrix in the former (Figure 3c). At 1.5 mm above the surface, the thus-fabricated and magnetized magnetoactive zone emitted an out-of-plane stray magnetic field component of 2.3 mT (±0.3 mT).

To demonstrate its applicability, a strip-shaped DCM valve (including a rectangular magnetoactive zone) was placed above a 5 V/400 mA powered electromagnet (Figure 3d). By applying a magnetic field using an electromagnet, the one-way valve closed and blue-stained water flowed through the valve. On turning off the field, the valve subsequently opened and the fluid flow stopped. The devices were also tested for actuation using a hard magnet. We observe that irrespective of the configuration, the actuation (switching) process is highly repeatable (>20×) with a negligible reduction in magnetic response.

Valve Actuation. For versatility, adoptability, and tunability, M-μPADS should be designed to be portable and user friendly. In an inhomogeneous magnetic field, the volumetric field gradient force on an object is given by

$$f_{\text{mag}} = (M\cdot\nabla)\boldsymbol{B}$$

Here, M is the magnetization vector of the object, in this case, the magnetoactive region of the valve, and $\boldsymbol{B}$ is the induction vector of the magnetic field source. Therefore, maximizing the field gradient optimizes the attractive force on the valve. It could be advantageous if the field source is electronically controlled (intensity or position) and operated at a low voltage, hence amenable to a processor-based control. As a field source, one could consider an electromagnet (as discussed above) or a permanent magnet.

The commonly used Arduino interface allows one to operate an electromagnet at a maximum of 5 V/400 mA, limiting the intensity of the magnetic field it can produce (Figure S3, measured using a Gaussmeter) and more severely, its magnetic field gradient induced by the coil would be limited to 0.8 T/m. Furthermore, the coil heats up (~40 °C), which might have some undesirable effects on the biochemical assays performed with the M-μPAD. These issues can be resolved by an appropriate choice of electromagnet size and its thermal management, which is however beyond the scope of this work. We, therefore, propose to fabricate valves using hard magnets. A NdFeB permanent magnet (Ø = 8 mm, height = 4 mm) provides 5 times greater field gradient (4.6 T/m Figure 4a) at the same working distance (3 mm) as the electromagnet discussed above. When the hard magnetic particles are

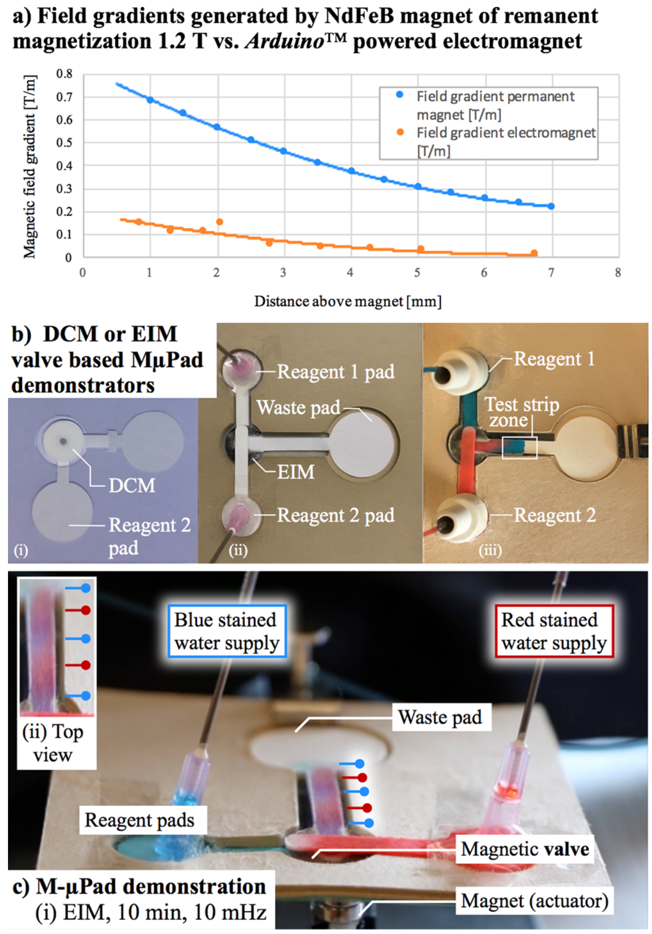

Figure 4. (a) Magnetic field gradient as a function of distance from the magnet. (b) Assembled two-inlet M-μPADS. (i) DCM valve assay and (ii) EIM valve assay. (iii) Result of switching valve from 1 to 2 in 120 s. (c) Demonstration of an M-μPAD with alternating reagents: (i) front view after 10 min, valve in neutral position and (ii) top view.

magnetized in the direction opposite to the magnetic field source, to produce a repulsive force (position 2), the maximum strength of the magnetic field source should be less than the coercive field value of the hard magnetic particles so as not to (partially) demagnetize the magnetoactive zones. The NdFeB hard magnetic particles used here have a coercive field value of about 0.8 T, whereas the field produced at 3 mm above the field source is 0.15 T (Figure S3), rendering the reduction in magnetization negligible.

To change the valve position, we mounted two permanent magnets (oriented in opposite directions) on a servo motor operated by an Arduino microcontroller (the exact setup and source code can be found in the Supporting Information and is shown in Figure S3). Three positions were programmed to operate the valve: position 1, valve open to the bottom channel (Figure 1), position 2, valve open to the top channel, and position 0, valve closed (in the latter case, no magnet was positioned under the valve). The opening of the valves after activation by an external magnetic field is quasi instantaneous. However, in the case of activation by an external permanent magnet, the latter must be positioned below the valve using the servo motor. Because of the lag in rotational movement, position switching of a valve operated with a motor is about 0.6 s, whereas the valve operated by electromagnets can be switched nearly instantaneously. However, the induced delay is

DOI: 10.1021/acsomega.7b01839
ACS Omega 2018, 3, 2049−2057

very reproducible as the motor always performs the same movement; thus, the delay can be considered during programming of the sequence. Finally, it is worth noting that this delay is very small compared to the average flow speed of the liquid in our paper structure (which, the experiment shows (Figure S4), is about 0.5 mm/s). The actuation speed of the valve is also influenced by paper properties; depending on the porosity and paper chemistry, more or less fluid can pass through the valve. A lighter paper can be operated with a lower magnetophoretic force, hence, less particles. Gravitational forces, however, will bend thinner paper toward position 1 when the channel is filled with a fluid. Furthermore, wetting this paper reduces its stiffness and smaller particle sizes are required for this region to remain embossed. In contrast, a stiffer paper may require higher forces to actuate a motion, but gravitational forces will have less effect on them. Finally, the retracting force of the paper valve must be greater than the capillary force between the wet surfaces to allow the valve to return to position 0 (closed).

Applications of Magnetic Two-Way Valves in a Sequential Fluid Delivery. The key advantages of two-way paper-based valves are hypothesized to be their capabilities to perform an automated, programmable, and controlled multistep liquid delivery especially from multiple inlets into a single outlet. This capability could garner applications in immunoassays where multiple wash steps or timed reagent additions are necessary. Conventional lateral flow immunoassays, for example, are limited to a single-step delivery of chemicals, without the capability to add washing, blocking steps, or signal amplifying reagents.[45−47] The automated addition of critical components onto highly sensitive assays such as enzyme-linked immunosorbent assays could significantly improve their limit of detection, lower contamination events, and boost reproducibility (hence reliability). Thus, we propose the incorporation of magnetoactive zones onto conventional paper-based PoC strips as a unique approach toward automated, multichannel, paper-based devices.

To demonstrate the applicability of these devices, we built an M-μPAD demonstration compatible with both magnetic valve techniques (DCM & EIM). First, a single source and drain channel configuration was fabricated using the DCM valve (Figure 4b(i)). In these devices, the valve acts as a timer, where the rate of wicking in the drain channel is slowed down by cutting off the supply. This is important where reagents are embedded in the paper and time is needed for a reaction to reach completion. Although we demonstrate the DCM valve with a single source and drain, this can be extended to two sources with the separation space acting as a neutral (0 point) and each reagent being designated as + or − relative to the z-axis.

In our EIM-based prototype, two reagent pads connected to a reservoir with syringe needles were used as the source with a channel that feeds into the valve and subsequently wicks to the drain channel Figure 4b(ii). The drain channel was terminated with a waste pad to ensure a continuous flow. Colored aqueous solutions were introduced into the device via a microfluidic syringe pump providing blue (reagent 1) and red (reagent 2) solutions at 0.01 mL s^{-1}. Because these devices are wicking-based, a pump-free configuration could also be set up, exploiting either capillary rise or gravity to deliver the dyes into the source channels and across the valve. In Figure 4b(iii), the valve was first opened toward reagent 1 (blue), which fills up the drain channel with the blue dye. After 120 s, the valve was switched toward reagent 2 (red), which allows the red dye to enter the test strip. Finally, the valve was closed toward position 0, which stops the fluid flow.

On the basis of the ability to switch between one source channel to another orthogonal to fluidic flow (along the z-axis), we envisioned that an array of blue-red color sequences (stripes) can be loaded into the drain channel by programming timed switching between the two source channels, making these devices a dynamic valve. To demonstrate the dynamic properties of this magnetic valve system, we recorded a sequence in which an EIM-M-μPAD was flipped between position 1 and 2 at a frequency of approximately 10 mHz. A video can be found in the Supporting Information (accelerated 20×) while Figure 4c shows a snapshot of a recording after 10 min. During this time, the valve switched six times between the two fluid supplies, providing a blue/red barcode-like channel coloring. The ability to sequentially add different liquids in a highly controlled manner could potentially open new applications in paper microfluidics, especially in the area of diagnostics,[24,48,49] bioenvironmental analysis,[50] or fabrication of neoteric platforms such as in infochemistry.[51,52] A minimum cycle of 20× was performed without change in performance. Also, an analysis of the fluid velocity depending on the valve position can be found in Figure S4.

While we demonstrate that EIM-based M-μPAD can create alternating blocks (red-blue), mixing of liquids was also achieved. Darcy's law predicts that the fluid pressure will drop in longer paper segments leading to a significant drop in the flow rate. We therefore hypothesized and demonstrated that the establishment of stripes of alternating colors depends on an equilibrium between the switching frequency and the wicking rate. When the switching frequency is sufficiently low, the source fluid significantly wicks away from the valve allowing the creation of band structures. When the switching frequency is significantly higher, it can be anticipated that the lateral displacement of the liquid into the drain channel will be insignificant; hence, the contact with a second fluid leads to mixing. By tuning the switching frequency, we can therefore induce mixing at different segments of the test strip and create separated bands as needed (purple color, Figure S5). At higher frequencies (0.1 Hz), we observed direct mixing in the valve entry regions. In this case, the primary (blue) fluid does not significantly wick into the drain channel before the introduction of the second reagent (red) leading to mixing (purple). Reagent mixing can also be controlled by changing the test strip length, as predicted by Darcy's law. We therefore infer that these valve systems are dynamic and tunable because the presence of bands or mixed states can be achieved by tuning the M-μPAD geometry, switching frequency, channel size, and viscous properties of the fluid.

Compared to previously reported paper-based valve systems, these magnetic two-way valves and associated M-μPADS have several advantages: (i) they are cyclic valves that can be opened or closed multiple times, (ii) the presented two-way valves are the first paper-based magnetic valves that possess a neutral position, two inlets and one outlet system, opening a new range of possibilities for making paper-based three-dimensional (3D) networks. These devices have a potential to adapt to multiple source channels. The valve can also be inverted, resulting in a one-inlet and two-outlet system, creating new opportunities for fluid separation, (iii) M-μPADS implemented here are based on programmable microprocessor electronics and therefore can be either triggered using human−machine interfaces, such as

DOI: 10.1021/acsomega.7b01839
ACS Omega 2018, 3, 2049−2057

buttons or other advanced interfaces such as touchscreens or operated autonomously based on a predefined procedure, and (iv) finally, M-μPADS come with full flexibility in design and fabrication, making their production amenable to large-industrial applications (DCM) or for smaller research and prototyping environments (EIM).

Despite their advantages, M-μPADS present two shortcomings: (i) the design relies on paper-based 3D multilayer [either open channel or wicking (so-called closed channel)[53] devices which are more complex to fabricate than classical two-dimensional paper devices. Nonetheless, there is now a large expertise in multilayer paper devices,[12,20,23,54] and their fabrication is becoming cheaper and more efficient compared to classical (open channel) microfluidic lab-on-chip devices. (ii) M-μPADS, by definition, require magnetic actuation either by electromagnets or permanent magnets, and both must be actuated by an electronic circuit. The price of these components is in strong contrast with the low costs of the paper components; however, recent evidence points toward efficiency rather than zero cost as the critical variable in PoC/use devices.[55] To mitigate lifetime cost of the devices, the magnets can be encapsulated and physisorbed onto the paper, allowing users to reuse the magnetoactive zones on different test strips, hence lowering the total cost of the devices, that is, the actuators are transferable from one device configuration to another. This could potentially lower both the fabrication cost and environmental impact, especially when using rare earth magnets. Such a design will, however, make the devices less user friendly, which is crucial in PoC devices. Furthermore, by combining the small-scale and wireless nature of such devices, they can be easily integrated into handheld devices such as the multidisease diagnostic devices recently developed by Liu and co-workers.[56,57] Overall, the devices reported herein have a significant potential in the development of pump-free microfluidics, as highlighted below.

Prospects. Flow in capillary microfluidics[29] and paper-based microfluidics[7,54] is often explained with the hydraulic−electric circuit where the resistance to flow corresponds to the electrical resistance, the volumetric flow rate to the electrical current, and the pressure drop to the potential drop. Classical microfluidic devices have been designed and developed in an analogous fashion to electronic components.[30] In paper-based microfluidics, Chen et al.[18] described the valves they presented as diodes because fluids can only flow through them in one direction. One-way paper magnetic valves[27] can also be compared to transistors as they can be (i) opened, (ii) closed, or (iii) regulate the amount of fluid flow through high-frequency open−close operations. In this analogy, the two-way paper magnetic valves described in this paper are analogous to both a transistor and also to a single-pole double-throw relay, allowing diversification of the device complexity beyond a simple switch. These valves are, therefore, logical operators that will likely open new capabilities in the near future.

Simplicity. Microfluidic devices embody the power of stackable and hackable simplicity and hence have a potential for a significant impact in research and technology development.[58,59] Gated microfluidic devices offer an opportunity to develop a diverse array of devices to address otherwise complex problems. The equivalence of a good microfluidic valve to a transistor or a switch embeds within it the potential for diversification into a complex system such as a computer network (best captured by the internet) albeit without the complexity of quantum phenomena in electronic devices. The magnetically actuated valves presented in this article can be easily stacked by the addition of multiple ports and valves to create multiple sources or drains. Furthermore, as previously described, our system is also highly customizable—"hackable" in terms of geometry, modulating frequency, and paper properties. Thus, we infer that the innovation conveyed here is a simple solution for the advancing field of wicking-based microfluidic devices.

■ CONCLUSION

The reported three-point magnetic valves allow for selective, programmable, and tunable delivery of fluids across a source and drain in a manner that can be adapted into more complex device structures. The fabrication is rapid, and devices are relatively efficient and low cost. Specifically, we demonstrated that

(i) two-way microfluidic valves can be fabricated with electromagnets or permanent magnets, and these devices can be tuned to form mixtures of separated plugs of different solutions;
(ii) by exploiting the well-known fluid transport in porous media, the capillary-driven flow properties of a liquid on a paper can be predicted and exploited to design an actuation scheme that leads to mixing or consecutive bands of solutions; and
(iii) the developed valves can be extended to more complex microfluidic device layouts to create elaborate bioanalytical platforms for effective and rapid sensing, diagnostics, or sample preparation.

■ MATERIALS AND METHODS

Materials. Gas-atomized NdFeB particles (MQP-S-11-9) were provided by Magnequench GmbH (Germany) and sieved to obtain an average size of 40 μm. These particles were magnetized under 1.5 T using a Harvey Wells (USA) electromagnet. All induced magnetic fields were measured using a Gaussmeter from FW Bell (USA) model 5080. The Arduino Uno R3 board, Grove electromagnet, servo motor, and all electronic components were obtained from Seeed Technology Co., Ltd (China). NdFeB magnets were obtained from supermagnete Webcraft GmbH (Germany). PDMS Sylgard 184 was obtained from Dow Corning and (1*H*,1*H*,2*H*,2*H*-perfluorooctyl)silane was purchased from Sigma-Aldrich. Duro Super Glue was purchased from the Iowa State University Chemistry Store. Food coloring was obtained from Ach Food Companies, Inc. All components were used as received. A cost approximation can be found in Table S6.

Experimental Methods. In general, all components of the 3D paper networks (M-μPADS, including EIM valve) were built using industrial blotting paper fabricated in-house. This cellulose fiber-based material was made from a mix of softwood and hardwood fibers, with no added fillers, on a pilot paper machine. This paper had a thickness of 493 ± 17 μm (micrometer Lhomargy (ISO 534:2011)) with a grammage of 287.4 g/m^2 (ISO 536:2012) and a porosity of 0.62 (by comparison with the fiber density of cellulose). This material has been shown to maintain its strength and rigidity under wet conditions.[60] The paper used for the DCM valves were produced using an ISO 5269-2:2005 (DIN 54 358) TAPPI process machine, a sheet former for the preparation of laboratory sheets of pulp.

DOI: 10.1021/acsomega.7b01839
ACS Omega 2018, 3, 2049−2057

All paper components (valves, structural components) were cut using a Cameo Omega 2, Silhouette America, Inc. (USA) craft cutter. The paper was embossed using 3D-printed (FlashForge 3D printer, dual extruder, USA) molds. To prevent any contact of the biological sample with the magnetic particles, a hydrophobic barrier was incorporated in certain valves between the magnetoactive zone and the capillary surface. To do this, we followed the procedure reported before by Oyola-Reynoso et al. on the TACH hand-drawn technique[61] (Figure S7). A sketch ball pen was used to deposit a hydrophobic "ink" composed of 5:1 v/v % of hexane and silane. The structural components of the M-μPAD device were modified chemically to prevent any leakage from the inlets. The modification was performed through chemical vapor deposition of silane.[62] In a clean and dry desiccator, precut paper samples were placed followed by 0.1 mL of alkylsilanes in a 10 mL dram vial. The desiccator was evacuated (~30 mm_{Hg} pressure), fixed, and placed in a preheated oven at 95 °C for 10 h. The M-μPADS were assembled using layers of paper and commercial tape.[3] Water dyed with food coloring (ACH Food Companies) was injected into M-μPADS using a Fusion 720 syringe pump by Chemyx, Inc. SEM was performed using FEI Inspect F50.

ASSOCIATED CONTENT

Supporting Information

The Supporting Information is available free of charge on the ACS Publications website at DOI: 10.1021/acsomega.7b01839.

Fixing magnetic micro-particles with superglue; additional information on magnetic actuation; fluid velocity during valve actuation; mixing of liquids; cost analysis data; drawing of hydrophobic barriers using TACH; and empirical and *in silico* flow behavior of dyed water in a paper channel (PDF)

Dynamic properties of M-μPad with alternating red- and blue-stained water (MPG)

AUTHOR INFORMATION

Corresponding Authors

*E-mail: jean-francis.bloch@3sr-grenoble.fr (J.-F.B.).

*E-mail: mthuo@iastate.edu (M.M.T.).

ORCID

Martin M. Thuo: 0000-0003-3448-8027

Notes

The authors declare no competing financial interest.

ACKNOWLEDGMENTS

This work was supported by Iowa State University through startup funds to M.M.T. M.M.T. acknowledges support from a Black and Veatch "Developing a world of difference" faculty fellowship. S.O.-R. was supported in part by a GMAP fellowship from Iowa State University. M.F. was supported by the French Ministry of Higher Education, Research and Innovation (MESRI, *bourse doctorale ministérielle*). Experiments were carried out at Iowa State University, CIME-Nanotec/FMNT, Grenoble INP Pagora and Institut Néel. The authors thank Orphée CUGAT and Victor VIEILLE for fruitful discussions.

REFERENCES

(1) Hawkins, K. R.; Weigl, B. H. Microfluidic Diagnostics for Low-Resource Settings. *Proc. SPIE* **2010**, *7593*, 75930L.

(2) Jung, W.; Han, J.; Choi, J.-W.; Ahn, C. H. Point-of-Care Testing (POCT) Diagnostic Systems Using Microfluidic Lab-on-a-Chip Technologies. *Microelectron. Eng.* **2015**, *132*, 46−57.

(3) Martinez, A. W.; Phillips, S. T.; Whitesides, G. M. Three-Dimensional Microfluidic Devices Fabricated in Layered Paper and Tape. *Proc. Natl. Acad. Sci. U.S.A.* **2008**, *105*, 19606−19611.

(4) Li, X.; Ballerini, D. R.; Shen, W. A Perspective on Paper-Based Microfluidics: Current Status and Future Trends. *Biomicrofluidics* **2012**, *6*, 11301−1130113.

(5) Liana, D. D.; Raguse, B.; Gooding, J. J.; Chow, E. Recent Advances in Paper-Based Sensors. *Sensors* **2012**, *12*, 11505−11526.

(6) Nery, E. W.; Kubota, L. T. Sensing Approaches on Paper-Based Devices: a Review. *Anal. Bioanal. Chem.* **2013**, *405*, 7573−7595.

(7) Yetisen, A. K.; Akram, M. S.; Lowe, C. R. Paper-Based Microfluidic Point-of-Care Diagnostic Devices. *Lab Chip* **2013**, *13*, 2210−2251.

(8) Hu, J.; Wang, S.; Wang, L.; Li, F.; Pingguan-Murphy, B.; Lu, T. J.; Xu, F. Advances in Paper-Based Point-of-Care Diagnostics. *Biosens. Bioelectron.* **2014**, *54*, 585−597.

(9) Coltro, W. K. T.; Cheng, C.-M.; Carrilho, E.; de Jesus, D. P. Recent Advances in Low-Cost Microfluidic Platforms for Diagnostic Applications. *Electrophoresis* **2014**, *35*, 2309−2324.

(10) Cate, D. M.; Adkins, J. A.; Mettakoonpitak, J.; Henry, C. S. Recent Developments in Paper-Based Microfluidic Devices. *Anal. Chem.* **2015**, *87*, 19−41.

(11) Mettakoonpitak, J.; Boehle, K.; Nantaphol, S.; Teengam, P.; Adkins, J. A.; Srisa-Art, M.; Henry, C. S. Electrochemistry on Paper-Based Analytical Devices: a Review. *Electroanalysis* **2016**, *28*, 1420−1436.

(12) Xia, Y.; Si, J.; Li, Z. Fabrication Techniques for Microfluidic Paper-Based Analytical Devices and Their Applications for Biological Testing: a Review. *Biosens. Bioelectron.* **2016**, *77*, 774−789.

(13) Fu, E.; Downs, C. Progress in the Development and Integration of Fluid Flow Control Tools in Paper Microfluidics. *Lab Chip* **2017**, *17*, 614−628.

(14) Koo, C. K. W.; He, F.; Nugen, S. R. An Inkjet-Printed Electrowetting Valve for Paper-Fluidic Sensors. *Analyst* **2013**, *138*, 4998−5004.

(15) Phillips, E. A.; Shen, R.; Zhao, S.; Linnes, J. C. Thermally Actuated Wax Valves for Paper-Fluidic Diagnostics. *Lab Chip* **2016**, *16*, 4230−4236.

(16) Jiang, Y.; Hao, Z.; He, Q.; Chen, H. A Simple Method for Fabrication of Microfluidic Paper-Based Analytical Devices and on-Device Fluid Control with a Portable Corona Generator. *RSC Adv.* **2016**, *6*, 2888−2894.

(17) Ainla, A.; Hamedi, M. M.; Güder, F.; Whitesides, G. M. Electrical Textile Valves for Paper Microfluidics. *Adv. Mater.* **2017**, *29*, 1702894.

(18) Chen, H.; Cogswell, J.; Anagnostopoulos, C.; Faghri, M. A Fluidic Diode, Valves, and a Sequential-Loading Circuit Fabricated on Layered Paper. *Lab Chip* **2012**, *12*, 2909−2913.

(19) Houghtaling, J.; Liang, T.; Thiessen, G.; Fu, E. Dissolvable Bridges for Manipulating Fluid Volumes in Paper Networks. *Anal. Chem.* **2013**, *85*, 11201−11204.

(20) Toley, B. J.; Wang, J. A.; Gupta, M.; Buser, J. R.; Lafleur, L. K.; Lutz, B. R.; Fu, E.; Yager, P. A Versatile Valving Toolkit for Automating Fluidic Operations in Paper Microfluidic Devices. *Lab Chip* **2015**, *15*, 1432−1444.

(21) Kong, T.; Flanigan, S.; Weinstein, M.; Kalwa, U.; Legner, C.; Pandey, S. A Fast, Reconfigurable Flow Switch for Paper Microfluidics Based on Selective Wetting of Folded Paper Actuator Strips. *Lab Chip* **2017**, *17*, 3621−3633.

(22) Li, B.; Yu, L.; Qi, J.; Fu, L.; Zhang, P.; Chen, L. Controlling Capillary-Driven Fluid Transport in Paper-Based Microfluidic Devices Using a Movable Valve. *Anal. Chem.* **2017**, *89*, 5707−5712.

(23) Martinez, A. W.; Phillips, S. T.; Nie, Z.; Cheng, C.-M.; Carrilho, E.; Wiley, B. J.; Whitesides, G. M. Programmable Diagnostic Devices Made From Paper and Tape. *Lab Chip* **2010**, *10*, 2499−2504.

DOI: 10.1021/acsomega.7b01839
ACS Omega 2018, 3, 2049−2057

(24) Fu, E.; Liang, T.; Spicar-Mihalic, P.; Houghtaling, J.; Ramachandran, S.; Yager, P. Two-Dimensional Paper Network Format That Enables Simple Multistep Assays for Use in Low-Resource Settings in the Context of Malaria Antigen Detection. *Anal. Chem.* **2012**, *84*, 4574−4579.
(25) Glavan, A. C.; Martinez, R. V.; Maxwell, E. J.; Subramaniam, A. B.; Nunes, R. M. D.; Soh, S.; Whitesides, G. M. Rapid Fabrication of Pressure-Driven Open-Channel Microfluidic Devices in Omniphobic RF Paper. *Lab Chip* **2013**, *13*, 2922−2930.
(26) Glavan, A. C.; Niu, J.; Chen, Z.; Güder, F.; Cheng, C.-M.; Liu, D.; Whitesides, G. M. Analytical Devices Based on Direct Synthesis of DNA on Paper. *Anal. Chem.* **2016**, *88*, 725−731.
(27) Li, X.; Zwanenburg, P.; Liu, X. Magnetic Timing Valves for Fluid Control in Paper-Based Microfluidics. *Lab Chip* **2013**, *13*, 2609−2614.
(28) Fu, E.; Ramsey, S. A.; Kauffman, P.; Lutz, B.; Yager, P. Transport in Two-Dimensional Paper Networks. *Microfluid. Nanofluid.* **2011**, *10*, 29−35.
(29) Oh, K. W.; Lee, K.; Ahn, B.; Furlani, E. P. Design of Pressure-Driven Microfluidic Networks Using Electric Circuit Analogy. *Lab Chip* **2012**, *12*, 515−545.
(30) Zhang, Q.; Zhang, M.; Djeghlaf, L.; Bataille, J.; Gamby, J.; Haghiri-Gosnet, A.-M.; Pallandre, A. Logic Digital Fluidic in Miniaturized Functional Devices: Perspective to the Next Generation of Microfluidic Lab-on-Chips. *Electrophoresis* **2017**, *38*, 953−976.
(31) Dempsey, N. M.; Le Roy, D.; Marelli-Mathevon, H.; Shaw, G.; Dias, A.; Kramer, R. B. G.; Cuong, L. V.; Kustov, M.; Zanini, L. F.; Villard, C.; Hasselbach, K.; Tomba, C.; Dumas-Bouchiat, F. Micro-Magnetic Imprinting of High Field Gradient Magnetic Flux Sources. *Appl. Phys. Lett.* **2014**, *104*, 262401.
(32) Le Roy, D.; Shaw, G.; Haettel, R.; Hasselbach, K.; Dumas-Bouchiat, F.; Givord, D.; Dempsey, N. M. Fabrication and Characterization of Polymer Membranes with Integrated Arrays of High Performance Micro-Magnets. *Mater. Today Commun.* **2016**, *6*, 50−55.
(33) Hamedi, M. M.; Campbell, V. E.; Rothemund, P.; Güder, F.; Christodouleas, D. C.; Bloch, J.-F.; Whitesides, G. M. Electrically Activated Paper Actuators. *Adv. Funct. Mater.* **2016**, *26*, 2446−2453.
(34) Oyola-Reynoso, S.; Heim, A. P.; Halbertsma-Black, J.; Zhao, C.; Tevis, I. D.; Çınar, S.; Cademartiri, R.; Liu, X.; Bloch, J.-F.; Thuo, M. M. Draw Your Assay: Fabrication of Low-Cost Paper-Based Diagnostic and Multi-Well Test Zones by Drawing on a Paper. *Talanta* **2015**, *144*, 289−293.
(35) He, Y.; Wu, Y.; Fu, J.-Z.; Wu, W.-B. Fabrication of Paper-Based Microfluidic Analysis Devices: a Review. *RSC Adv.* **2015**, *5*, 78109−78127.
(36) Malekghasemi, S.; Kahveci, E.; Duman, M. Rapid and Alternative Fabrication Method for Microfluidic Paper Based Analytical Devices. *Talanta* **2016**, *159*, 401−411.
(37) Carrilho, E.; Martinez, A. W.; Whitesides, G. M. Understanding Wax Printing: a Simple Micropatterning Process for Paper-Based Microfluidics. *Anal. Chem.* **2009**, *81*, 7091−7095.
(38) Jeong, S.-G.; Lee, S.-H.; Choi, C.-H.; Kim, J.; Lee, C.-S. Toward Instrument-Free Digital Measurements: a Three-Dimensional Microfluidic Device Fabricated in a Single Sheet of Paper by Double-Sided Printing and Lamination. *Lab Chip* **2015**, *15*, 1188−1194.
(39) Tenda, K.; Ota, R.; Yamada, K.; Henares, T.; Suzuki, K.; Citterio, D. High-Resolution Microfluidic Paper-Based Analytical Devices for Sub-Microliter Sample Analysis. *Micromachines* **2016**, *7*, 80.
(40) Masoodi, R.; Pillai, K. M. Darcy's Law-Based Model for Wicking in Paper-Like Swelling Porous Media. *AIChE J.* **2010**, *56*, 2257−2267.
(41) Schuchardt, D. R.; Berg, J. C. Liquid Transport in Composite Cellulose - Superabsorbent Fiber Networks. *Wood and Fiber Science*; The Society, 1991; pp 342−357.
(42) Koponen, A.; Kandhai, D.; Hellén, E.; Alava, M.; Hoekstra, A.; Kataja, M.; Niskanen, K.; Sloot, P.; Timonen, J. Permeability of Three-Dimensional Random Fiber Webs. *Phys. Rev. Lett.* **1998**, *80*, 716−719.
(43) Lucas, R. Ueber Das Zeitgesetz Des Kapillaren Aufstiegs Von Flüssigkeiten. *Kolloid Z.* **1918**, *23*, 15−22.
(44) Washburn, E. W. The Dynamics of Capillary Flow. *Phys. Rev.* **1921**, *18*, 273−283.
(45) Fu, E.; Kauffman, P.; Lutz, B.; Yager, P. Chemical Signal Amplification in Two-Dimensional Paper Networks. *Sens. Actuators, B* **2010**, *149*, 325−328.
(46) Posthuma-Trumpie, G. A.; Korf, J.; van Amerongen, A. Lateral Flow (Immuno)Assay: Its Strengths, Weaknesses, Opportunities and Threats. a Literature Survey. *Anal. Bioanal. Chem.* **2009**, *393*, 569−582.
(47) Fu, E.; Liang, T.; Houghtaling, J.; Ramachandran, S.; Ramsey, S. A.; Lutz, B.; Yager, P. Enhanced Sensitivity of Lateral Flow Tests Using a Two-Dimensional Paper Network Format. *Anal. Chem.* **2011**, *83*, 7941−7946.
(48) Ramachandran, S.; Fu, E.; Lutz, B.; Yager, P. Long-Term Dry Storage of an Enzyme-Based Reagent System for ELISA in Point-of-Care Devices. *Analyst* **2014**, *139*, 1456−1462.
(49) Abadian, A.; Manesh, S. S.; Ashtiani, S. J. Hybrid Paper-Based Microfluidics: Combination of Paper-Based Analytical Device (μPAD) and Digital Microfluidics (DMF) on a Single Substrate. *Microfluid. Nanofluid.* **2017**, *21*, 65.
(50) Park, J.; Shin, J. H.; Park, J.-K. Pressed Paper-Based Dipstick for Detection of Foodborne Pathogens with Multistep Reactions. *Anal. Chem.* **2016**, *88*, 3781−3788.
(51) Kim, C.; Thomas, S. W.; Whitesides, G. M. Long-Duration Transmission of Information with Infofuses. *Angew. Chem., Int. Ed.* **2010**, *49*, 4571−4575.
(52) Hashimoto, M.; Feng, J.; York, R. L.; Ellerbee, A. K.; Morrison, G.; Thomas, S. W.; Mahadevan, L.; Whitesides, G. M. Infochemistry: Encoding Information as Optical Pulses Using Droplets in a Microfluidic Device. *J. Am. Chem. Soc.* **2009**, *131*, 12420−12429.
(53) Thuo, M. M.; Martinez, R. V.; Lan, W.-J.; Liu, X.; Barber, J.; Atkinson, M. B. J.; Bandarage, D.; Bloch, J.-F.; Whitesides, G. M. Fabrication of Low-Cost Paper-Based Microfluidic Devices by Embossing or Cut-and-Stack Methods. *Chem. Mater.* **2014**, *26*, 4230−4237.
(54) Osborn, J. L.; Lutz, B.; Fu, E.; Kauffman, P.; Stevens, D. Y.; Yager, P. Microfluidics Without Pumps: Reinventing the T-Sensor and H-Filter in Paper Networks. *Lab Chip* **2010**, *10*, 2659−2665.
(55) Kimani, F.; Mwangi, S.; Kwasa, B.; Kusow, A.; Ngugi, B.; Chen, J.; Liu, X.; Cademartiri, R.; Thuo, M. Rethinking the Design of Low-Cost Point-of-Care Diagnostic Devices. *Micromachines* **2017**, *8*, 317.
(56) Zhao, C.; Thuo, M. M.; Liu, X. A Microfluidic Paper-Based Electrochemical Biosensor Array for Multiplexed Detection of Metabolic Biomarkers. *Sci. Technol. Adv. Mater.* **2013**, *14*, 054402.
(57) Zhao, C.; Thuo, M. M.; Liu, X. Microfluidic Paper-Based Multiplexing Biosensors for Electrochemical Detection of Metabolic Biomarkers. In *Microfluidic Methods for Molecular Biology*; Lu, C., Verbridge, S. S., Eds.; Springer International Publishing: Cham, 2016; pp 205−218.
(58) Tian, X.; Lind, K. R.; Yuan, B.; Shaw, S.; Siemianowski, O.; Cademartiri, L. Simplicity as a Route to Impact in Materials Research. *Adv. Mater.* **2017**, *29*, 1604681.
(59) Whitesides, G. M. *Towards a Science of Simplicity*; TED, 2010.
(60) du Roscoat, S. R.; Decain, M.; Thibault, X.; Geindreau, C.; Bloch, J.-F. Estimation of Microstructural Properties From Synchrotron X-Ray Microtomography and Determination of the REV in Paper Materials. *Acta Mater.* **2007**, *55*, 2841−2850.
(61) Oyola-Reynoso, S.; Frankiewicz, C.; Chang, B.; Chen, J.; Bloch, J.-F.; Thuo, M. M. Paper-Based Microfluidic Devices by Asymmetric Calendaring. *Biomicrofluidics* **2017**, *11*, 014104.
(62) Oyola-Reynoso, S.; Tevis, I. D.; Chen, J.; Chang, B. S.; Çinar, S.; Bloch, J.-F.; Thuo, M. M. Recruiting Physisorbed Water in Surface Polymerization for Bio-Inspired Materials of Tunable Hydrophobicity. *J. Mater. Chem. A* **2016**, *4*, 14729−14738.

DOI: 10.1021/acsomega.7b01839
ACS Omega 2018, 3, 2049−2057